# Preparation of MgO Thin Film by Neutral Beam Assisted Deposition as a Protective Layer of AC PDP

***Zhao-Hui Li and Sang Jik Kwon****
**Dept. of Electronics Engineering, Kyungwon University, Seongnam City, Kyunggi 461-701, Korea**
*TEL: +82-31-750-5319, e-mail: sjkwon@kyungwon.ac.kr*

**Keywords: PDP, MgO, NBAD**

## Abstract

*In this experiment, MgO thin films were deposited by oxygen neutral beam assisted deposition (NBAD) method. The results show that neutral beam energy plays an important role in the surface morphology, crystal orientation, defects of MgO thin films, and discharge characteristics of AC PDP*

## 1. Introduction

Plasma display panels (PDPs) are expected to be one of the most promising candidates for use in large-sized high-definition televisions (HDTV), because of their advantages of occupying small space, wide viewing angle, and low weight. [1] A protective layer of AC PDPs plays an important role in lowering the discharge voltage and protecting the dielectric layer from ion bombardments during gas discharge. MgO thin film is widely used as a protective layer for AC PDP owing to its high secondary electron emission coefficient (γ), low sputtering yield, and high durability. [2]

Electron beam (E-bam) evaporation is one of the technologies used for depositing the MgO thin film as an AC PDP protective layer. During MgO deposition by E-beam evaporation, however, the MgO is decomposed into Mg and O atoms, and then the decomposed Mg and O atoms arrive at the substrate, building up one by one, and are finally re-crystallized as MgO [3]. Many research studies have shown the discharge characteristics of PDP and the structural properties of MgO thin films, which were deposited by e-beam evaporation with respect to oxygen ($O_2$) or hydrogen ($H_2$) flow rate. The secondary electron emission is very sensitive to the nature of the MgO thin film, such as its surface morphology, film density, crystal orientation, and surface roughness. [4-6]

In this experiment, we deposited MgO thin films by oxygen neutral beam assisted deposition (NBAD) method. And we investigated the characteristics of MgO thin films and the discharging properties of AC PDP.

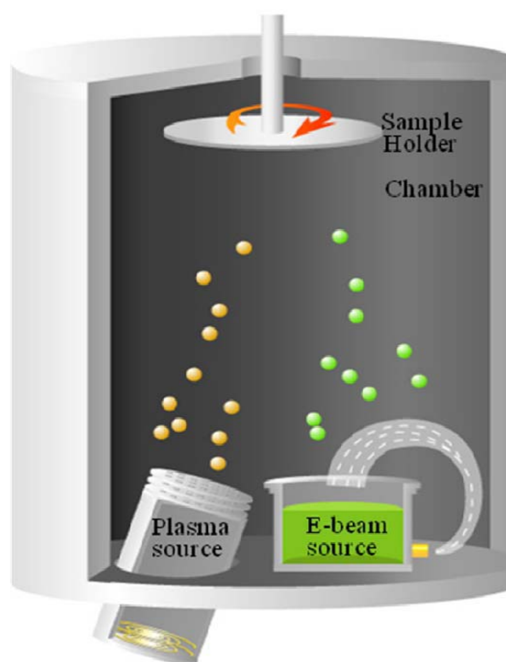


**Fig. 1. Schematic diagram of NBAD system.**

We investigated the characteristics of MgO thin films deposited by oxygen neutral beam assisted deposition method (NBAD) when the assisting neutral beam energy was varied from 100 to 700 eV.

## 2. Experimental

First, 2-inch test panels were prepared on the substrate of PDP glass (PD200). The thickness of the address electrode was approximately 8 ㎛ and the width was approximately 200 ㎛. The thickness of

the dielectric layer was approximately 24 ㎛, and the barrier rib height was approximately 130 ㎛. The green phosphor was coated using the screen printer and its thickness was approximately 10 ㎛. The width of the bus electrodes was approximately 80 ㎛ and the height was approximately 8 ㎛. Moreover, the MgO layer was deposited using an NBAD method.

A schematic diagram of the NBAD system is shown in Fig. 1. The oxygen (99.99%) flow was fixed at 10 sccm, and the plasma was created using an RF ion source. The power of the RF ion source was 200 W. The vacuum chamber was evacuated to a base pressure of $2\times10^{-6}$ torr and the working pressure was $3.6\times10^{-5}$ torr. The deposition temperature was 300℃, and the deposition rate was ~5 Å/s. At the same time, one sample (No NBAD) was prepared by only e-beam evaporation without neutral beam irradiation for comparison. Annealing and aging processes were carried out before the discharging test was performed. The discharge gas Ne + Xe (4%) was filled to 400 torr in the test chamber. A 50 kHz square pulse was used to drive the PDP test panels.

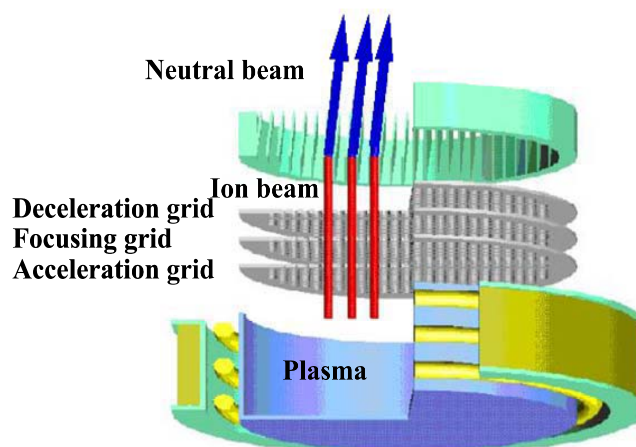


**Fig. 2 Schematic diagram of neutral beam source.**

Neutral beam is usually used in the semiconductor process. In this experiment, neutral beam was generated using an ion gun and a low-angle reflector. [7, 8] Figure 2 shows a schematic of our neutral beam source. In this neutral beam source, plasma is created using an RF plasma source, and voltage applied to the accelerated grid control the neutral beam energy, and the voltage is varied from 100 to 700 eV. The deceleration grid is connected to the ground, and the voltage applied to the focusing grid is 0 V. Thus, only positive ions pass through the hole in the grids. They are accelerated toward the low-angle reflectors and are neutralized by a resonance neutralization process and an Auger capture process using the low-angle reflector. [9]

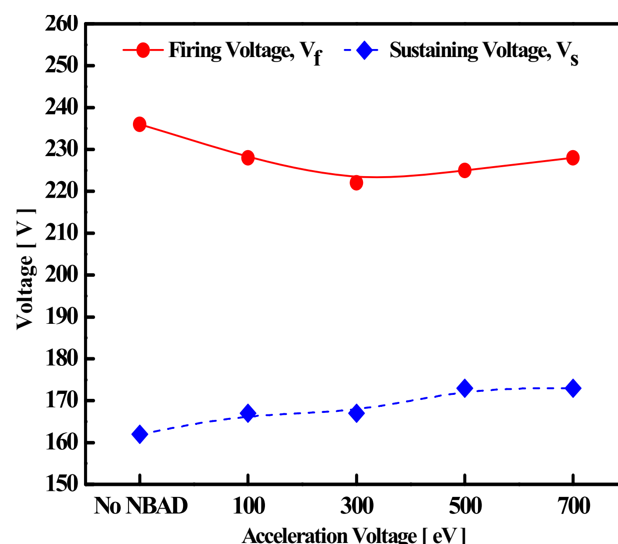


**Fig. 3. Firing voltage ($V_f$) and sustain voltage ($V_s$) of PDP with the MgO protective layer deposited by NBAD.**

In addition, the firing inception voltage ($V_f$) and the sustaining voltage ($V_s$) were measured using a current probe (Tektronix TCPA300) and an oscilloscope (Tektronix TDS-540C). X-ray diffraction (XRD), scanning electron microscopy (SEM), and cathode luminance (CL) spectrometer were employed to investigate the crystal orientation and properties of the MgO thin films, respectively.

## 3. Results and discussion

The plots of firing inception voltage ($V_f$) and sustaining voltage ($V_s$) are shown in Fig. 3. Here, $V_f$ is defined as the voltage when all the pixels are turned on. $V_s$ is the voltage when the first cell is turned off form the ON state. The $V_f$ is minimum when the neutral beam energy is 300 eV. The $V_f$ decreases with increasing neutral beam energy from 100 to 300 eV, which is clearly lower than that of the No NBAD sample. However, when the neutral beam energy is over 300 eV, the $V_f$ increases with the increasing neutral beam energy. On the other hand, $V_s$ values always increase with the neutral beam increase from 100 to 700 eV, which is higher than that of the No NBAD sample. According to the Paschen law, the

secondary electron emission coefficient (γ) is inversely proportional to $V_f$. Thus, we can say that the maximum secondary electron emission coefficient is obtained at the neutral beam energy of 300 eV in this experiment.

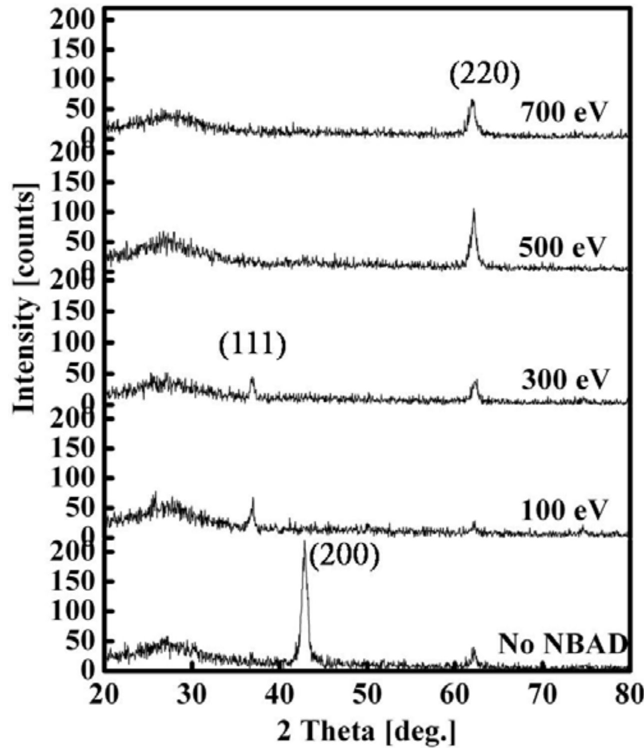


**Fig. 4. XRD spectrum of MgO thin film deposited by NBAD.**

Figure 4 shows the XRD spectra of MgO thin films deposited with varying neutral beam energies. The No NBAD MgO thin film, which was deposited by only e-beam evaporation without oxygen gas inputting or neutral beam assisting, has (200) and (220) preferred orientations. The MgO thin films deposited by NBAD have no (200) preferred orientation. The MgO thin films deposited by NBAD have (220) preferred orientation and their peak intensity varied depending on the neutral beam energies. In the relatively low-energy range from 100 to 300 eV, (220) peaks were predominant and their intensity was maximum at the neutral beam of 300 eV. On the other hand, in the energy ranges higher than 500 eV, (111) peak becomes disappearance again. We consider that the variation of the preferred orientation and the peak intensity results from the neutral beam energy. However, detailed investigations on the effects of preferred orientation of MgO thin film on the secondary electron mission are in process.

Figure 5 shows the SEM micrographs of the MgO thin films deposited by NBAD method. It is distinct that the surface morphology of the MgO thin films varied with neutral beam energy. The No NBAD MgO thin film has larger grains. However, the MgO thin film grain becomes finer and smaller when the neutral beam is assisted. From 100 to 500 eV, the grain size decreases with the neutral beam energy increasing. However, when the neutral beam energy is 700 eV, the grain size becomes much larger than anyone. And the shape of grain also becomes triangular. On the other hand, the gap between grains also increases with the neutral beam energy increasing.

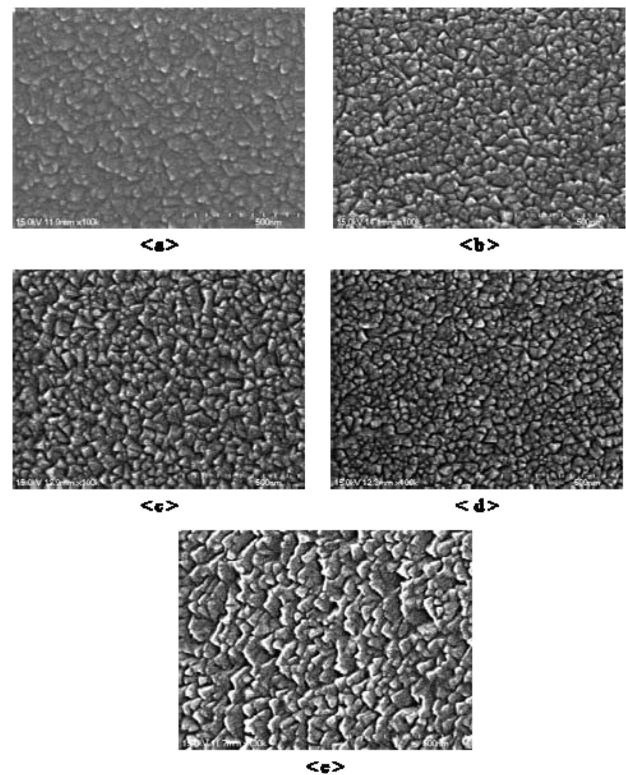


**Fig. 5. SEM micrographs of MgO thin film deposited by NBAD method: (a) No NBAD, (b) 100 eV, (c) 300 eV, (d) 500 eV and (e) 700 eV.**

The defects of MgO thin films play an important effect on the discharge of AC PDP. As mentioned in introduction section, the $F/F^+$ centers always are present in the MgO thin films deposited by conventional E-beam evaporation. In order to analyze the $F/F^+$ centers of MgO thin films under different neutral beam energy, we measured CL spectra of the MgO thin films using CL spectrometer. Figure 6 shows the CL spectra of the MgO thin films deposited

by NBAD. It is well known that the CL intensity is proportional to the intensity of the $F/F^+$ centers. As shown in Fig. 6, the No NBAD has the highest CL peak. And the CL peak intensity decreases with the neutral beam energy increasing. We can estimate that, as the neutral beam energy increases, the oxygen atoms impinging on the substrate increase and, therefore, the $F/F^+$ centers of the MgO film reduces.

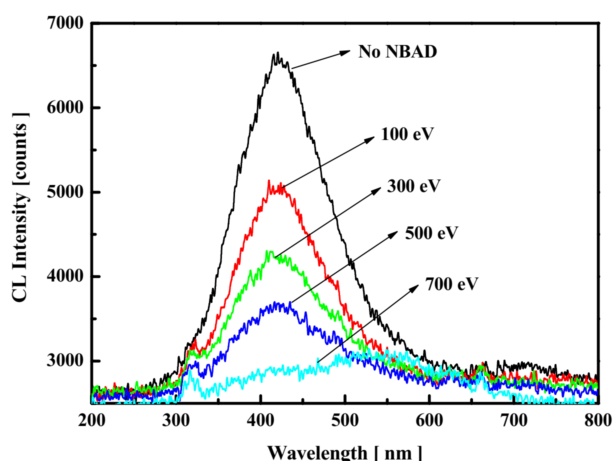


**Fig. 6. CL spectrum of MgO thin film deposited by NBAD method.**

It is well known that the discharge characteristic of AC PDP is very sensitive to the nature of its MgO protective layer, such as its surface morphology, structural characteristics and so on. From Figs. 3 and 5, when the grain of MgO thin film is finer, the MgO thin film has higher SEE yield and higher discharge luminescence. The $F/F^+$ centers have a direct effect on the discharge characteristics of AC PDP, however, this relationship between the $F/F^+$ centers and the discharge characteristics is not clear in this study.

## 4. Summary

In a summary, the oxygen neutral beam energy affects significantly the surface morphology and the structural properties of MgO thin films, resultantly the discharge characteristics of PDP. In our experiment, the most desirable properties of MgO thin films were obtained for the sample that was deposited with the neutral beam energy of 300 eV. The maximum SEE yield was obtained when the neutral beam energy was 300 eV. Otherwise, the preferred orientation and the surface morphology of MgO thin film also varied with the different neutral beam energy. And the intensity of the $F/F^+$ centers decrease with the neutral beam energy increasing. When the neutral beam energy is over 700 eV, the MgO thin film has almost $F/F^+$ centers

## 5. References

1. M. Ishimoti, R. Baragiola, and T. Shinoda, *IDW'00 Techncial Digest*, p. 683 (2000).
2. R. H. Kim, Y. H. Kim, and J. W. Park, *J. Vac. Sci. Technol. A*, **18**, 2493 (2000).
3. Y. Ushio, T. Banno, N. Matuda, Y. Saito, B, Baba, and A. Kinbara, *Thin Solid Films*, **167[1-2]**, 299 (1988).
4. I. Koiwa, T. Kanehara, and J. Mita, *J. Electrochem. Soc.*, **142[5]**, 1396 (1995).
5. C. Y. Son, J. H. Cho, and J. W. Park, *J. Vac. Sci. Technol. A*, **17[5]**, 2619 (1999).
6. K. H. Park and Y. S. Kim, *IDW'06 Technical Digest*, Vol. **1**, p. 351 (2006).
7. D. H. Lee, J. W. Bae, S. D. Park, and G. Y. Yeom, *Thin Solid Films*, **398-399**, 647 (2001).
8. M. S. Hur, S. J. Kim, H. S. Lee, J. K. Lee, and G. Y. Yeom, *IEEE Trans. Plasma Sci.*, **30[1]**, 110 (2002).
9. S. J. Kim, H. J. Lee, G. Y. Yeom, and J. K. Lee, *Jpn. J. Appl. Phys.*, **43[10]**, 7261 (2004).